Absence of quantum diffusion in two-dimensional short coherence length superconductors

1993 J. Phys.: Condens. Matter 5 697

(http://iopscience.iop.org/0953-8984/5/6/006)

J. Phys.: Condens. Matter 5 (1993) 697–706. Printed in the UK

Absence of quantum diffusion in two-dimensional short coherence length superconductors

V C Hui and C J Lambert
School of Physics and Materials, Lancaster University, Lancaster LA1 4YB, UK

Received 5 June 1992, in final form 16 November 1992

Abstract. A numerical technique is used to demonstrate that excitations of a two-dimensional superconductor of length N and finite width M are localized by spatial fluctuations in the magnitude of the order parameter $\Delta(r)$. Results obtained using numerical finite size scaling, are consistent with the presence of a line of critical points in two dimensions. No such behaviour is found in the presence of phase fluctuations only.

1. Introduction

There are many situations in which the order parameter $\Delta(r)$ of a superconductor varies randomly in the space, even though the underlying normal potential is perfectly ordered. One example is provided by the melting of a flux lattice [1–3] in an otherwise perfectly crystalline high T_c superconductor [4]. Another should occur in anisotropic superconductors, where by analogy with ^{3}He–A, disordered textures can arise when an anisotropic phase is nucleated from a more symmetric phase such as ^{3}He–B.

In a high T_c superconductor, the coherence length ξ, which sets the scale for spatial fluctuations in $\Delta(r)$, is of the order of the size of a unit cell. Therefore, in order to describe the properties of quasi-particle excitations in such systems, it is necessary to go beyond effective medium treatments of the disorder. In one dimension, this was carried out for the first time in [5] where it was demonstrated that fluctuations in a superconducting order parameter alone can localize excitations, even at energies high above the bulk energy gap. In this paper, we address the question of whether or not this new phenomenon of superconductivity induced Anderson localization persists in higher dimensions.

At first sight, the answer to this question would appear to be in the affirmative. Preliminary calculations using a numerical finite size scaling approach [6] which suggested that localization in two dimensions does indeed occur, were followed by analytic work by Kravtsov and Oppermann [7] and by Zeigler [8], who found that in the presence of time reversal symmetry, states of energy $E = 0$ are localized for dimensions $d \leqslant 2$, while in the absence of time reversal symmetry, such states are localized in all dimensions. However, the results of [6] were obtained using rather small system sizes, while those of [7] used models constrained to have a finite density of states at $E = 0$. In an attempt to provide firmer evidence for superconductivity induced Anderson localization in two dimensions, we now report

0953-8984/93/060697+10$07.50

the results of extensive numerical simulations, performed on long strips of finite width.

2. Models of disorder

To address the question of superconductivity induced Anderson localization, we make use of the Bogoliubov–de Gennes (BG) equation

$$\begin{pmatrix} -\nabla^2 - 1 & \Delta(r) \\ \Delta^*(r) & \nabla^2 + 1 \end{pmatrix} \begin{pmatrix} \psi(r) \\ \phi(r) \end{pmatrix} = E \begin{pmatrix} \psi(r) \\ \phi(r) \end{pmatrix}. \tag{1}$$

Here all energies are measured in units of chemical potential $\mu = \hbar^2 k_F^2/2m$ and all length in units of k_F^{-1}. $\psi(r)$ are the particle and hole components of an excited state of energy E. In what follows, we regard $\Delta(r)$ as given, at least in a probabilistic sense. For the purpose of numerical computation, we discretize the Laplacian in equation (1) by introducing, in two dimensions, a square lattice with sites of separation a and positions r_j. On such a lattice, equation (1) becomes

$$(1/a^2)(2\psi(r_j) - \psi(r_{j-1}) - \psi(r_{j+1})) - \psi(r_j)\phi(r_j) = E\psi(r_j) \tag{2a}$$

$$-(1/a^2)(2\phi(r_j) - \phi(r_{j-1}) - \phi(r_{j+1})) + \psi(r_j) + \Delta^*(r_j)\psi(r_j) = E\phi(r_j). \tag{2b}$$

In this manner, discretization of equation (1) yields a nearest neighbour tight binding model with two degrees of freedom per site, coupled by an 'on site' particle–hole scattering element $\Delta(r_j)$. Provided $a \ll 1$ and the energy E lies well below the artificial upper band edge introduced by discretization, the properties of equation (1) will be faithfully reproduced.

Having placed the problem on a lattice, the aim now is to extract generic localization properties in two dimensions. For this purpose, we examine a lattice in which the order parameter $\Delta_j \exp(i\theta_j)$ on a given site j, varies randomly from site to site in an uncorrelated manner. As in the earlier work [5,6], two models will be considered, the first of which is invariant under time reversal, while the second is not. In model 1, $\theta_j = 0$ for all j, but Δ_j is uniformly distributed over the interval $\Delta_0(1 \pm \delta\Delta)$. In model 2, $\Delta_j = \Delta_0$ for all j, whereas θ_j is uniformly distributed in the range $\pm\delta\theta$. In what follows, the choice $\Delta_0 = 1$ and $a = \sqrt{0.1}$ is made. Since we are concerned with the generic properties we have moved away from the physical limit ($\Delta_0 \sim 1/a$) to gain computational efficiency ($a < 1$). If localization for such a discrete model can be demonstrated, an appeal to universality gives one confidence that localization will be present in more realistic models.

For a long strip of N slices, each containing M sites, and for a given E and realization of $\Delta(r_j)$, we employ the decimation method [9–11] to compute off-diagonal elements of the Green function $G_{i,j}(N, M)$ between degrees of freedom i on slice 1 and j on slice N. Since each site has a particle and hole degree of freedom, $G_{i,j}(N, M)$ is a $(1M)^2$ complex matrix. If angular brackets denote an ensemble average over the disorder, then the inverse localization length α_M is defined by

$$\alpha_M = \lim_{N\to\infty} \alpha_{M,N}$$

where

$$\alpha_{M,N} = -(4NM^2)^{-1}\left\langle \sum_{i,j=1}^{2M} \ln|G_{i,j}(M,N)| \right\rangle. \tag{3}$$

Of course it is well-known that excitations with energy E below the disorder free order parameter Δ_0 can form bound states due to Andreev scattering inside the cores of vortices [12] and that an excitation entering a homogeneous superconductor with $E < \Delta_0$ will be totally reflected [13]. However, such behaviour is a consequence of the presence of a gap in the density of states at these energies. To demonstrate localization in the Anderson sense, we must show that on average $G_{i,j}(M,N)$ decays exponentially with N, even for energies within the energy band. Therefore, in what follows, a node counting technique is incorporated into the decimation method, as described in [14], so that both α and the density of states of a system are obtained simultaneously.

Once exponential localization on strips of finite width M has been demonstrated, information about the two-dimensional limit can be obtained by plotting graphs of $\alpha_M M$ versus M [10,11]. For a given energy and disorder, if the slope of such a graph is positive, then a scale change decreases the transmission probability for an excitation and therefore states at that energy are localized. If the slope is negative, then the states are extended. The case of graphs possessing a vanishing slope is marginal and in practice, more difficult to interpret. Such behaviour has been found numerically [10] for the two-dimensional Anderson model with weak disorder and has been attributed to the possible existence of a line of critical points. It is consistent with the presence of extended states, for which the smallest Lyapunov exponent decreases as $1/M$. In practice such behaviour may also be indistinguishable from a slow logarithmic increase in $\alpha_M M$ with M, which is indicative of power law localization.

3. Results

For model 1, figure 1 shows the density of states per site $N(E)$ of long strips of width M = 10, 30, 50, for 9 disorders in $\Delta(r)$ ranging from $\delta\Delta$ = 0.1 to 0.9. Figure 2 shows the corresponding results for model 2 with disorder in the phase of $\Delta(r)$ ranging from $\delta\Theta = 0.1\pi$ to 0.9π. In these calculation strips of length $N \sim 10^3$ were used. Since the density of states is a self-averaging quantity, no change in the computed value of $N(E)$ was obtained by further increasing N. In practice, the node counting technique [14] yields the integrated density of states $I(E)$ at a chosen energy E. Figures 1 and 2 were obtained by computing $I(E)$ at energy intervals of spacing ΔE, and then defining $N(E) = (I(E+\Delta E) - I(E))/\Delta E$. For model 1, E ranges from 0.8 to 1.2 in steps of ΔE = 0.05, whereas for model 2, E ranges from 0.0 to 1.2 in steps of ΔE = 0.1. For superconductors with a homogeneous order parameter ($\Delta(r) = \Delta_0$) there is a square root singularity in the density of

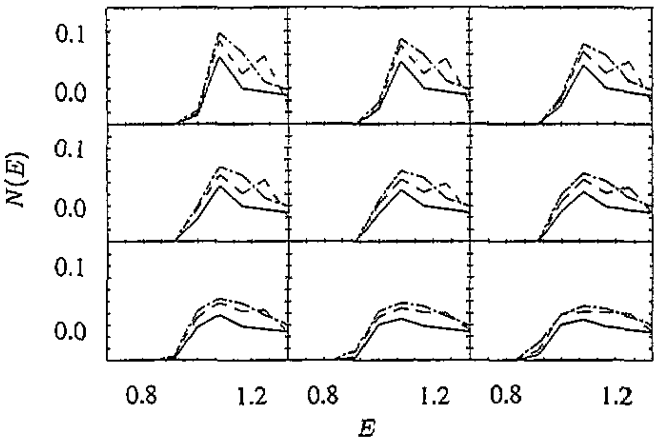

Figure 1. The density of states of model 1 for nine disorders $\delta\Delta$ starting from 0.1 (top left graphs) to 0.9 (bottom right graphs) in steps of 0.1. In each graph, (——), (- - -) and (— · —) correspond to strips of width M = 10, 30 and 50 and length N is 10^3.

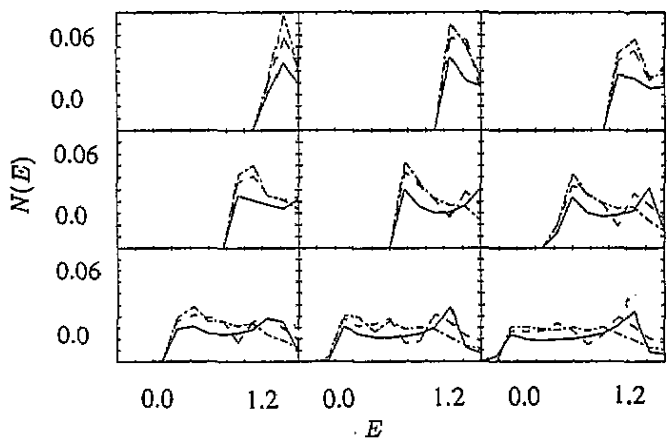

Figure 2. The density of states of model 2 for nine disorders $\delta\Delta$ running from 0.1π (top left graphs) to 0.9π (bottom right graphs) in steps of 0.1π. In each graph, (——), (- - -) and (— · —) correspond to strips of width M = 10, 30 and 50 and length N is 10^3.

states at energy $E = \Delta_0$. In the presence of disorder, figures 1 and 2 show that the singularity is suppressed and the energy gap is decreased through the presence of a Lifshitz tail.

Apart from the highest disorder results of model 2, figures 1 and 2 show that there is an energy $E_0 > 0$, below which no positive energy states are found numerically. For a system of width M and length N, this means that for $0 < E < E_0$, $N(E) < (NM)^{-1}$. At present no theory exists for the form of $N(E)$ at these energies. However for model 1, setting $\Delta(r) = \Delta_0(1 - \delta\Delta)$ for all r yields a lower bound of $E_{\min} = \Delta_0(1 - \delta\Delta)$. For model 2, a crude estimate of the cut-off in the density of states can be obtained by noting that for a homogeneous

superconductor in the presence of a superflow v, the excitation spectrum is of the form

$$E = v \cdot k + \sqrt{(k^2 - 1)^2 + |\Delta_0|^2} \tag{5}$$

which yields a lower bound of $E = \Delta_0 - v$. Since v is equal to the gradient of the phase of $\Delta(r)$, we find that for model 2, $v \leqslant 2\delta\theta/a$. Hence $E_{\min} = \Delta_0 - 2\delta\theta/a$. Both of these estimates of $E_{\min}$ are lower than the computed values of E_0, which suggests that although states at $E = E_{\min}$ are possible, the probability of occurrence of such states is small.

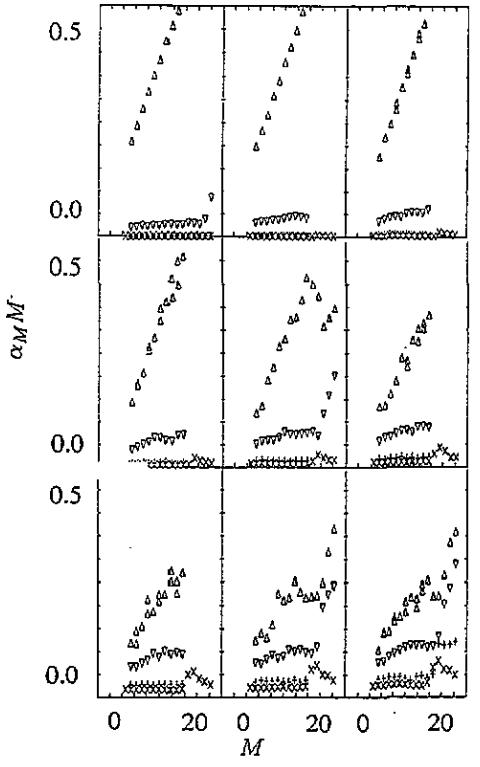

Figure 3. Plots of $\alpha_M M$ versus M for model 1, for nine disorders $\delta\Delta$ starting from 0.1 (top left) to 0.9 (bottom right). Points (Δ), (∇), (+) and (×) correspond to E = 0.975(Δ), 1.0(∇), 1.05(+) and 1.1(×). $N = 10^5$ in all cases.

To investigate the localization properties of excitated states we follow a standard finite size scaling technique [10,11] and plot graphs of $\alpha_M M$ versus M for various excitation energies E and disorders in $\Delta(r)$. The results, which are shown in figure 3 for model 1 and figure 4 for model 2, were obtained using strips of length $N = 10^5$. For model 1, we concentrate our effort on states in the band tails, at energies E = 0.975, 1.0, 1.05 and 1.1. For model 2, results for a range of E from 0.0 to 1.0 are shown and for both models, M varies from 5 to 20.

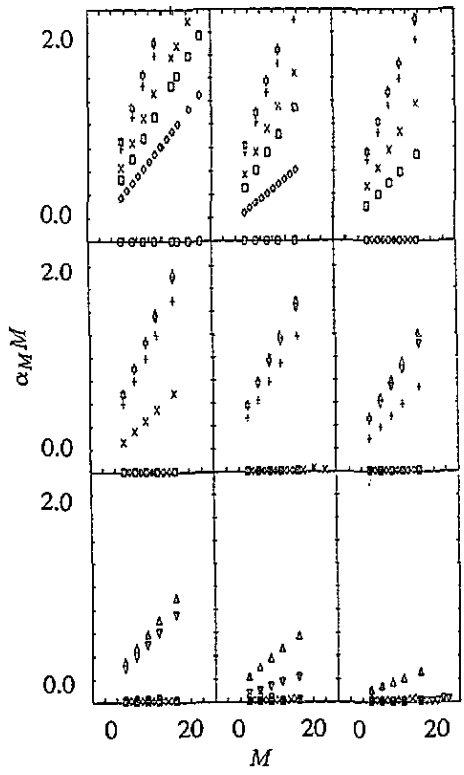

Figure 4. Plots of $\alpha_M M$ versus M for model 2 for nine disorders $\delta\Theta$ running from 0.1π (top left) to 0.9π (bottom right). Points (Δ), (∇), (+), (×), ($\Box$), ($\Diamond$) and ($\circ$) correspond to $E = 0.0$, 0.2, 0.4, 0.7, 0.8, 0.9 and 1.0. $N = 10^5$ in all cases.

First, we discuss the results for model 1 contained in figure 3, which shows nine graphs of $\alpha_M M$ versus M corresponding to nine disorders $\delta\Delta$ running from 0.1 to 0.9. Apart from notable irregularities at $M = 15$, the results show that there is a tendency for the product $\alpha_M M$ to increase with M for all chosen values of E and $\delta\Delta$, suggesting that the states are localized. These results are similar to those reported in [6]. However, the irregularities appearing at $M \sim 15$ suggest that the scaling regime may not yet have been reached. To check this possibility, values of $\alpha_M M$ were computed for widths up to $M = 100$ and the three disorders $\delta\Delta = 0.5$, 0.8, 0.9. These results are shown in figure 5 and reveal that the linear relationships between $\alpha_M M$ and M for $M < 20$ turn into the behaviour $\alpha_M M \simeq$ constant for $M > 20$. The horizontal lines are drawn as guides to the eye. This conclusion is more convincing if the same set data is plotted in graphs of α_M versus $1/M$. These results are shown in figure 6 and demonstrate an apparent linear relationship between α_M and $1/M$, with a gradient which increases with decreasing E as well as increasing $\delta\Delta$.

While the linear relationship between $\alpha_M M$ and M suggests localization, $\alpha_M M$ = constant is consistent with a line of critical points. On such a line, for large N $\alpha(M, N)N \sim N/M$, which shows that off-diagonal elements $G_{i,j}(M, N)$ typically decay exponentially with the aspect ration N/M. As noted above, this behaviour is reminiscent of that found for the Anderson model in two dimensions at low

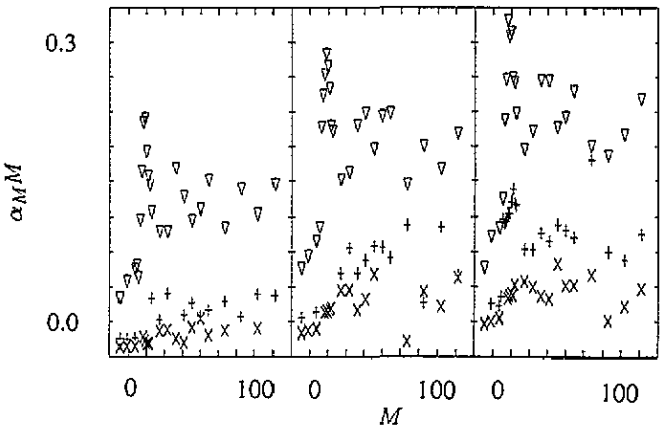

Figure 5. $\alpha_M M$ versus M for model 1, disorder $\delta\Delta = 0.5$ (left), 0.8 (middle) and 0.9 (right). Points (∇), (+) and (×) correspond to $E = 1.0$, 1.05 and 1.1. $N = 10^5$ in all cases.

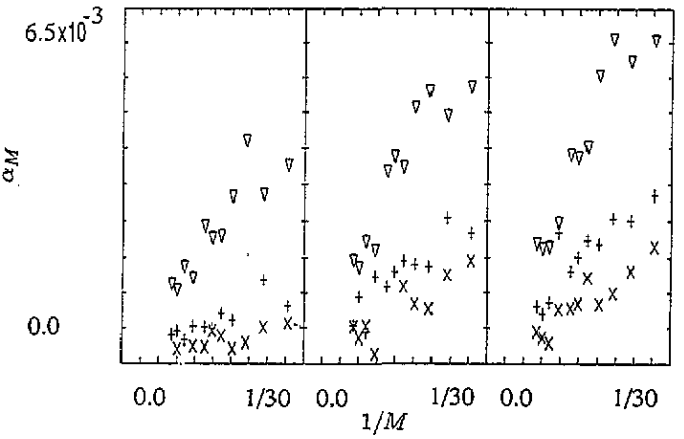

Figure 6. Using the same set of data in figure 5 for model 1 but plotting α_M against $1/M$.

disorder [10].

Results for model 2 are given in figure 4, which shows that linear relationships between $\alpha_M M$ and M with finite gradients can also occur for all disorders $\delta\theta$ ranging from 0.1π to 0.9π. However the density of states for this model, shown in figure 2, reveals that this behaviour occurs only for energies within a gap in the density of states. Hence the increase of $\alpha_M M$ with M simply reflects the decaying behaviour of the evanescent states within the gap. This also explains why, as the disorder increases and the band edge moves to lower energies, the number of curves in figure 4 exhibiting this behaviour decreases with increasing $\delta\Theta$.

For all states outside the gap in the density of states, $\alpha_M M$ shows no obvious trend as M increases. Indeed for such states, $\alpha_M \sim 1/N$, suggesting that even an exponential dependence on the aspect ratio does not arise for model 2. Figure 7

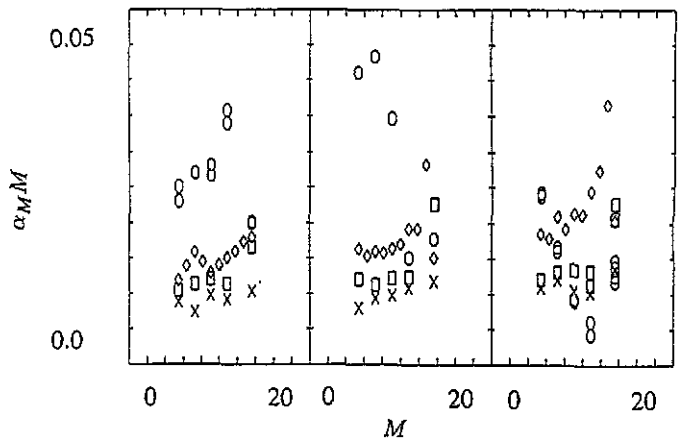

Figure 7. Using the same set of data in figure 4 for model 2 of disorder $\delta\Theta = 0.5\pi$, 0.8π and 0.9π but only the results of non-evanescent states are shown. Points (×), (□), (◇) and (○) correspond to $E = 0.7$, 0.8, 0.9 and 1.0. Maximum M is 20. $N = 10^5$ in all cases.

shows a selection of data used in figure 4 but without the results corresponding to evanescent states. Figure 8 shows results up to $M = 60$ for the strongest disorder $\delta\theta = 0.9\pi$. Unlike the results of figure 5, which clearly show non-zero limiting values of $\alpha_M M$, no such conclusion can be drawn from figure 8.

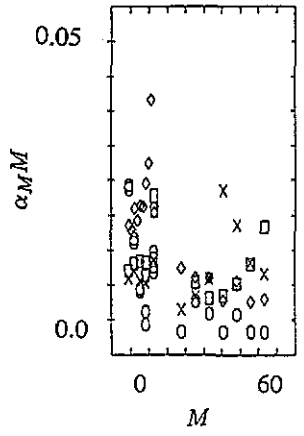

Figure 8. $\alpha_M M$ versus M for large M for model 2 with disorder $\delta\Theta = 0.9\pi$ and $N = 10^5$.

4. Discussion

The results reported in this paper are the end product of a large scale computational effort, involving vectorized code running for approximately 10^3 CPU hours on an Amdahl VP1200. The results obtained from model 1, demonstrate that excitations

on a long strip of superconductor are localized due to disorder in the magnitude of the order parameter $\Delta(r)$ and therefore the phenomenon of superconductivity induced Anderson localization should be present in real superconducting wires. In contrast, firm numerical evidence for the occurrence of localization in square samples has not been obtained. For model 1, which preserves time reversal symmetry, the results are consistent with a line of critical points. For model 2, which breaks time reversal symmetry, the scaling behaviour is consistent with the absence of Anderson localization.

These results are consistent with the trend found in normal disordered systems, where the breaking of time reversal symmetry tends to delocalize states. Furthermore, they show that the presence of an energy gap enhances the possibility of Anderson localization. As noted in section 2, in regions of a depressed order parameter, Andreev scattering can lead to the formation of discrete bound states at energies below the bulk gap. The enhancement of localization in the presence of a gap suggests that the continuum of localized states found by our simulations, may arise from the hybridization of such bound states.

It should be emphasized that the question of self-consistency and effects due to external magnetic fields, have not been addressed in this paper. In any real physical system, diagonal and off-diagonal fluctuations in the Bogoliubov–de Gennes equation will be correlated and it is of interest to ask if these correlations enhance or diminish quasi-particle localization. For the purpose of merely establishing the existence of superconductivity induced Anderson localization in two dimensions, we feel justified in neglecting such complications, but for the purpose of comparing results with real experiments, such effects should be included. To emphasize that order parameter fluctuations provide a new mechanism for localization, we have avoided including normal potential fluctuations in the models discussed in this paper. For the future, in order to gain more insight into superconductivity induced localization, we intend to investigate models incorporating both kinds of disorder and to examine trends in scaling behaviour as the normal disorder is decreased.

Acknowledgments

This work is supported by the SERC and the EC Science programme.

References

[1] Gammel P L, Bishop D J, Dolan G J, Kwo J R, Murray C A, Schneemeyer L F and Waszczak J V 1987 *Phys. Rev. Lett.* **59** 2592
[2] Houghton A, Pelcovits R A and Sudbo A 1989 *Phys. Rev.* B **40** 6763
[3] Moore M A 1989 *Phys. Rev.* B **39** 136
[4] In the first of these examples, the order parameter is not quenched. Nevertheless, close to the melting curve, the time scale for changes in $\Delta(r)$ can be made arbitrarily long and therefore in the spirit of the Born–Oppenheimer approximation, it is reasonable to freeze the disorder and to ask what changes this induces in the quasi-particles of such a system.
[5] Hui V C and Lambert C J 1990 *J. Phys.: Condens. Matter* **2** 7303
[6] Lambert C J and Hui V C 1990 *Physica* B **165** 1107
[7] Kravtsov V E and Oppermann R 1991 *Phys. Rev.* B **43** 10865
[8] Ziegler K 1991 *Z. Phys.* B **86** 33
[9] Lee P A and Fisher D 1981 *Phys. Rev. Lett.* **47** 882

[10] Pichard J L and Sarma G 1981 *J. Phys. C: Solid State Phys.* **14** L127 and L617
[11] Makinnon A 1981 *Localisation, Interaction and Transport Phenomena* ed B Kramer, G Bergmann and Y Bruynseraade (Springer)
[12] see for example
de Gennes P G 1966 *Superconductivity of Metals and Alloys* (New York: Benjamin)
[13] Andreev A F 1964 *Sov. Phys.–JETP* **19** 1228
[14] Lambert C J and Hughes G D 1991 *Phys. Rev. Lett.* **66** 1074